ACS APPLIED MATERIALS & INTERFACES

RESEARCH ARTICLE

www.acsami.org

Sensing of Digestive Proteins in Saliva with a Molecularly Imprinted Poly(ethylene-*co*-vinyl alcohol) Thin Film Coated Quartz Crystal Microbalance Sensor

Mei-Hwa Lee,[†] James L. Thomas,[‡] Hong-Yi Tseng,[†] Wei-Che Lin,[†] Bin-Da Liu,[§] and Hung-Yin Lin*[,⊥]

[†]Department of Materials Science and Engineering, I-Shou University, Kaohsiung 840, Taiwan

[‡]Department of Physics and Astronomy, University of New Mexico, Albuquerque, New Mexico 87131, United States

[§]Department of Electrical Engineering, National Cheng Kung University, Tainan 701, Taiwan

[⊥]Department of Chemical and Materials Engineering, National University of Kaohsiung, Kaohsiung 81148, Taiwan

Supporting Information

ABSTRACT: The quartz crystal microbalance (QCM) has a sensitivity comparable to that of the surface plasmon resonance (SPR) transducer. Molecularly imprinted polymers (MIPs) have a much lower cost than natural antibodies, they are easier to fabricate and more stable, and they exhibit satisfactory recognition ability when integrated onto sensing transducers. Hence, MIP-based QCM sensors have been used to recognize small molecules and, recently, microorganisms, but only a few have been adopted in protein sensing. In this work, a mixed salivary protein and poly(ethylene-*co*-vinyl alcohol), EVAL, solution is coated onto a QCM chip and a molecularly imprinted EVAL thin film formed by thermally induced phase separation (TIPS). The optimal ethylene mole ratios of the commercially available EVALs for the imprinting of amylase, lipase and lysozyme were found to be 32, 38, and 44 mol %, respectively. Finally, the salivary protein-imprinted EVAL-based QCM sensors were used to detect amylase, lipase and lysozyme in real samples (saliva) and their effectiveness was compared with that of a commercial ARCHITECT *ci* 8200 chemical analysis system. The limits of detection (LOD) for those salivary proteins were as low as ~pM.

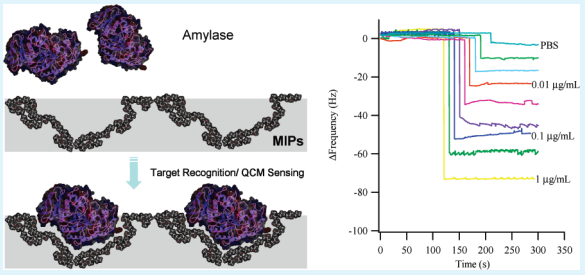

KEYWORDS: molecular imprinting, quartz crystal microbalance, salivary proteins, poly(ethylene-*co*-vinyl alcohol)

INTRODUCTION

The literature on three major applications of molecularly imprinted polymers: separation,[1,2] biosensing,[3,4] and delivery,[5] are briefly reviewed here. As early as the end of 1980s, much of the emphasis on molecularly imprinted polymers was shifting from purely theoretical or "proof of principle" work to sensing applications; the early development of this field saw interest in the use of electrodes and electrochemical measurements, motivated by work on the sensing capabilities of biomembranes on such electrodes.[6] Since 1995, several investigations have utilized acoustic transducers, such as quartz crystal resonators, sometimes integrated with molecularly imprinted polymers (MIP-QCM sensor), to measure either the mass change or the increased damping when molecules are adsorbed on their surfaces. Ávila et al. reviewed the use of molecularly imprinted polymers for the selective piezoelectric sensing of small molecules.[7] Recently, Dickert's group developed the sensing of microorganisms (such as yeast[8] and picornaviruses[9]), pollen[10] and even erythrocyte ABO subgroups.[11] Chou's group demonstrated the sensing of protein (such as albumin) using MIP-QCM.[12] Our earlier work demonstrated the recognition of a protein by exploiting microcontact imprinting with a monomer mixture[13] and with poly(ethylene-*co*-vinyl alcohol).[14] The widespread use of biological macro-templates (e.g., proteins) is reviewed by Ge and Turner.[15] Poly(ethylene-*co*-vinyl alcohol) has also been used for imprinting proteins and smaller molecules and for forming composite nanoparticles with either quantum dots[16] or magnetic nanoparticles,[17] for the electrochemical,[18] optical,[16] and magnetic sensing of template molecules[17] in biological fluids (especially urine). Although the electrochemical sensing of biomarkers using molecularly imprinted polymers has the advantage of requiring only low-cost equipment,[18] the limit of detection may be not sufficiently low for most important biomarkers in biological fluids.

The functions of saliva include tasting, bolus formation, buffering, protection against demineralization, remineralization, lubrication, digestion, as well as antiviral, antifungal and antibacterial protection.[19] The main components that are involved in digestion are amylase, protease, lipase, deoxyribonuclease and ribonuclease. Salivary amylase is also called ptyalin and acts on

Received: May 9, 2011
Accepted: July 7, 2011
Published: July 07, 2011

linear α(1,4)glycosidic linkages of starch to yield maltose and dextrin. A decline in the concentration or activity of amylase may be caused by oral cancer, cardiovascular disease and the smoking of tobacco. The median activity of salivary amylase in oral squamous cell carcinoma (OSCC) patients was insignificantly lower, by 25%, than that of reference concentration (p = 0.12).[20] Endothelial lipase gene in OSCC-derived cell lines is found downregulated for −4.98 ± 0.70 folds.[21] Salivary amylase activity was determined before and 6 h after cardiovascular surgery. Low salivary amylase levels in preoperative patients with ruptured aortic aneurysm are associated with increased mortality.[22,23] Cigarette smokers have significantly reduced salivary amylase activity.[24] Salivary amylase concentration is also measured to evaluate the damage to salivary glands during radiotherapy in the treatment of head and neck cancer.[19,25] In the mixed saliva of the oral squamous cell carcinoma patients, the lysozyme concentration was significantly increased (p = 0.011).[26] Salivary lysozyme was also reported may associate with coronary artery disease (CAD).[27,28]

In this work, salivary proteins with digestive functions (such as amylase, lipase, and lysozyme) were imprinted using a biocompatible polymer, poly(ethylene-*co*-vinyl alcohol). The feasibility of the noncovalent recognition of target proteins by molecularly imprinted polymers and the thermal induced phase separation (TIPS) formation of molecularly imprinted polymer thin films were also examined. Incorporating molecularly imprinted polymers in a quartz crystal microbalance is a highly sensitive method for the "label-free" measurement of salivary proteins on the molecularly imprinted thin films.

MATERIALS AND METHODS

Reagents. α-Amylase (EC 3.2.1.1, Cat. No. 10080, 43.6 U/mg) and lipase (EC 3.1.1.3, Cat. No. 62300, powder, 15−35 U/mg), both from hog pancreas, and lysozyme (EC 3.2.1.17) from hen egg white were purchased from Fluka Biochemika (Buchs, Switzerland). Poly(ethylene-*co*vinyl alcohol), EVAL, with ethylene 27, 32, 38, and 44 mol % (product no. 414077, 414093, 414085, 414107) were from Sigma-Aldrich Co. (St. Louis, MO). Dimethyl sulfoxide (DMSO, product # 161954) was purchased from Panreac (Barcelona, Spain) and used as the solvent to dissolve EVAL polymer particles in the concentration of 1 wt %. Absolute ethyl alcohol was from J. T. Baker (ACS grade, NJ). Sodium dodecyl sulfate (SDS) was purchased from Sigma-Aldrich Co. (St. Louis, MO) and used for the removal of target molecules. All chemicals were used as received unless otherwise mentioned.

Formation of Salivary Protein-Imprinted Poly(ethylene-*co*vinyl alcohol) Thin Film. The synthesis of salivary protein-imprinted (amylase-imprinted, lipase-imprinted and lysozyme-imprinted) and nonimprinted EVAL thin film included three steps (as shown in scheme 1(a)): (A) dissolving target proteins in various imprinting concentrations in DMSO and adding granular EVAL to the protein/DMSO solution to form clear EVAL solution (EVAL/DMSO = 1.0 wt %); (B) solidification of the thin film by placing the sample in the oven for five minutes until solvent evaporates; and then (C) removal of the template molecule by washing with 20 mL deionized water 10 min for two times. The nonimprinted polymer (NIP) thin films were prepared identically, except that the template protein was omitted.

"Preliminary" (prescreening) binding measurements of target molecules to the imprinted or nonimprinted EVAL thin films can be found elsewhere[18] and were made to determine optimal compositions. These measurements were performed by adding

Scheme 1. (a) Preparation of Amylase-Imprinted Poly(ethylene-co-vinyl alcohol) and (b) Possible Recognition Mechanism of Amylase on a QCM Chip

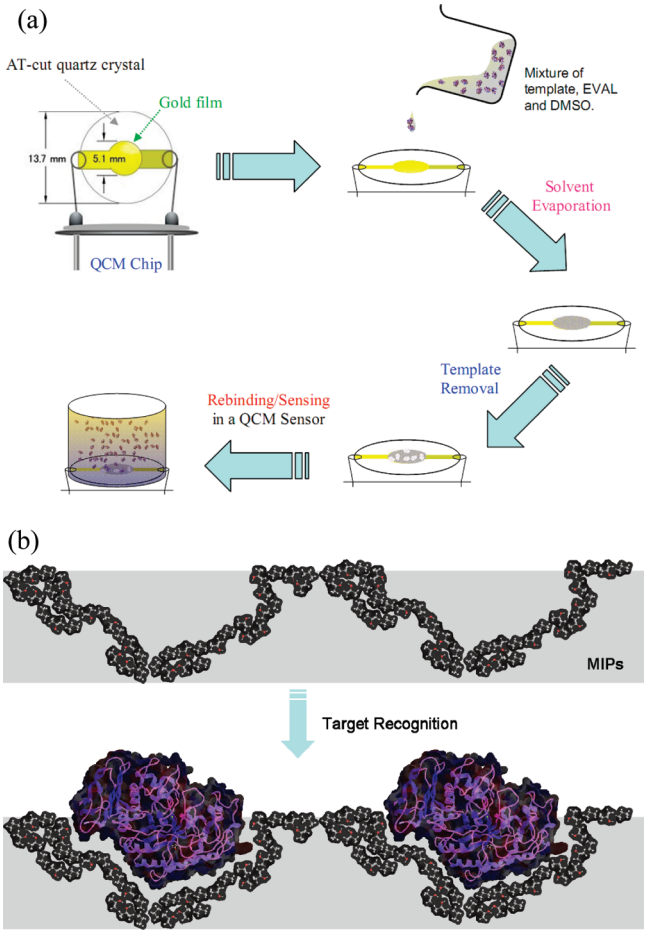

2 mL of buffer containing 0.1 mg/mL target molecules (unless otherwise stated) to MIP and NIP films for 30 min. The depletion of template from the buffer was assayed by a UV/vis spectrometer (Lambda 40, PerkinElmer, Wellesley MA), as determined by absorbencies of target molecules (amylase: 265 nm; lipase: 260 nm and lysozyme: 280 nm).

Surface Characterization of Salivary Protein-Imprinted Poly(ethylene-*co*vinyl alcohol) Thin Film. The water contact angle measurements were performed with a video-based optical contact angle meter (model 100SL, Sindatek Instruments Co. Ltd.). Protein-imprinted EVAL thin films were dried with nitrogen gas. A 4 μL droplet of deionized water was then placed on the polymeric thin film, and the contact angle measured by video imaging, using the "circle method".[29]

The oxygen, nitrogenm and carbon atomic percentages on the EVAL MIP thin films were also measured by X-ray photoelectron spectroscopy (Axis Ultra DLD, Kratos Analytical, Manchester, England); the results are shown in the Supporting Information. We found that nitrogen concentration before template removal, after template removal, and after target rebinding were 1.11, 0.48, and 0.91, respectively, for amylase-MIPs. The changes show that washing removes some, but not all, of the template molecules. We cannot rule out the possibility that some surface molecules remain permanently bound; however, the permanently bound

Table 1. Prescreening of Template Molecules to the Molecular Imprinting and Nonimprinting Poly(ethylene-*co*-ethylene alcohol) Thin Films and Their Imprinting Effectiveness on Different Ethylene Mol % of EVALs[a]

	amylase adsorption (μg/cm^2)			lipase adsorption (μg/cm^2)			lysozyme adsorption (μg/cm^2)		
EVAL (ethylene mol %)	MIP	NIP	IF	MIP	NIP	IF	MIP	NIP	IF
27	16.16 ± 3.51	12.97 ± 2.70	1.25	10.94 ± 0.12	13.65 ± 0.16	0.80	6.83 ± 0.78	3.33 ± 0.78	1.30
32	**22.03 ± 0.54**	**9.46 ± 0.15**	**2.28**	19.27 ± 0.86	12.35 ± 0.47	1.56	10.56 ± 1.09	6.36 ± 0.31	1.28
38	[b]3.53 ± 1.84	[b]5.61 ± 2.97	0.63	**23.57 ± 0.14**	**10.53 ± 0.26**	**2.13**	14.99 ± 0.47	9.63 ± 0.78	1.85
44	17.83 ± 0.37	10.67 ± 1.97	1.67	20.88 ± 3.03	11.82 ± 0.07	1.77	**21.99 ± 0.93**	**8.93 ± 0.31**	**2.47**

[a] MIP: Molecular imprinting polymer; NIP: Non-imprinting polymer; IF: Imprinting effectiveness. [b] See comment in the Figure 1 caption.

templates do not prevent the use of these films for the QCM sensing, as we show.

Atomic force microscopy of the molecularly imprinted polymers was also performed using with NT-MDT Solver P47H-PRO AFM, (Moscow, Russia). Images were made in air (room temperature (ca. 27 °C) and 87% relative humidity) using the tapping mode with scan rate 0.75 Hz. The cantilever was a SiO_2 probe (model: TGS1, NT-MDT, Moscow, Russia) with 2 nm probe tip size and 144 kHz resonant frequency.

Frequency Monitoring of Protein Adsorption and Salivary Sample Measurement on the Imprinted EVAL QCM chip. The QCM chip (7.995 MHz, ALS, Japan) was immersed in 20 mL of 1N NaOH solution, DI water, 1N HCl solution, and DI water, successively (10 min for each step), and then washed with ethanol and DI water and dried with nitrogen gas. Please note that the EVAL solution is diluted 50 times (i.e., 0.02 wt %) prior to coating on the QCM chip to enhance the sensitivity. The amylase-, lipase-, and lysozyme- and nonimprinted polymers coated on a QCM chip were placed in the sensing chamber with 2 mL of PBS and then monitored with a QCM sensor (405A, CH Instruments, USA). Twenty microliters of various concentrations of amylase, lipase, and lysozyme in 2 mL of PBS were then added to the Teflon sensing chamber to plot the calibration curves. Salivary samples were secreted by our colleagues 10 min after rinsing the mouth and 4 h before the test. In general, 5−10 mL of saliva can be collected and centrifuged at 6000 rpm for 10 min. Seven hundred microliters of the salivary supernatant sample was also stored in an eppendorf microcentrifuge tube at 4 °C and analyzed with ARCHITECT *ci* 8200 system (Abbott Laboratories. Abbott Park, Illinois, U.S.A.) at E-Da Hospital. Twenty microliters of salivary samples were then added to the 2 mL sensing chamber for the measurement of resonant frequency shift due to the binding of target molecules to the molecularly imprinted EVAL thin films.

RESULTS AND DISCUSSION

Recently developed biosensors, based on such nanotechnology as optical (surface plasmon resonance, SPR) and mass sensitive (such as bulk acoustic wave resonator, BAW) transducers, have the potential to exhibit extremely high sensitivity even at low (pM) concentrations. Typically, natural antibodies or ligands for the target molecules are conjugated on the surface of the sensing chip. Issues of stability, availability and expense can make the use of natural antibodies as the sensing element problematic. The self-assembly of ligands on a chip surface may cause nonspecific binding and increase noise. Accordingly, the integration of low-cost and highly selective materials into highly sensitive transducers may provide an economical means of monitoring human health.

The noninvasive monitoring of human health and the diagnosis of disease and its progression are the most important problems that can be solved by the aforementioned approach. Many biomarkers in urine (such as sarcosine[30] and alanine[31]) have recently been statistically correlated with prostate cancer and elevated blood pressure. While urine is the biological fluid that is secreted in the largest amount, saliva may be the second most secreted biological fluid. Streckfus and Bigler[23] have reviewed the many studies of the use of saliva as a diagnostic fluid, used for example, in diagnosing autoimmune, cardiovascular, and endocrine disorders; viral, bacterial, renal, pharmacological, and psychiatric diseases, and cancer.

Table 1 depicts the binding capability of the imprinted EVAL thin films we prepared, assayed by measuring the depletion of target molecules in buffer by UV/vis spectroscopy. This prescreening of EVALs for various target molecules provides a rapid and facile approach for determining optimal preparation protocols, including the optimal mole percent of ethylene.[13,14] When amylase is used as the target molecule, the adsorption on (or in) EVAL thin films is as high as 22.03 ± 0.54 μg/cm^2 (Table 1). EVAL with 32 mol % of ethylene has a higher imprinting effectiveness than other ethylene ratios, which makes it more promising for the formation of amylase-imprinted EVAL thin film on a QCM chip. For lipase imprinting, the adsorption capacity first increases with an increasing ethylene mole ratio, reaching a maximum at 38 mol % with an adsorption capacity of 23.57 ± 0.14 μg/cm^2 and an imprinting effectiveness of 2.13. This composition was chosen for later integration with the QCM for sensing. The third target protein used for imprinting is lysozyme, which is also found in saliva in a low concentration. The batch adsorptions of lysozyme to lysozyme-imprinted EVAL thin films linearly increases from 6.83 ± 0.78 to 21.99 ± 0.93 μg/cm^2 when the mole ratio of ethylene increases from 27 to 44 mol %. For nonimprinted EVAL thin films, the highest adsorption capacity for lysozyme was always less than 10 μg/cm^2, and lower ethylene mol % resulted in lower adsorption as shown in Figure 1.

We note that all of these absorption levels (including nonspecific binding on NIPs) are quite high, higher than could be achieved with monolayer coverage. There are two possible reasons for this: first, a substantial amount of the target may absorb nonspecifically to the vessel in which the MIPs and NIPs are tested. Second, especially for imprinted films, the films may be highly porous with large openings. (This is especially likely if the template molecules undergo any degree of self-association

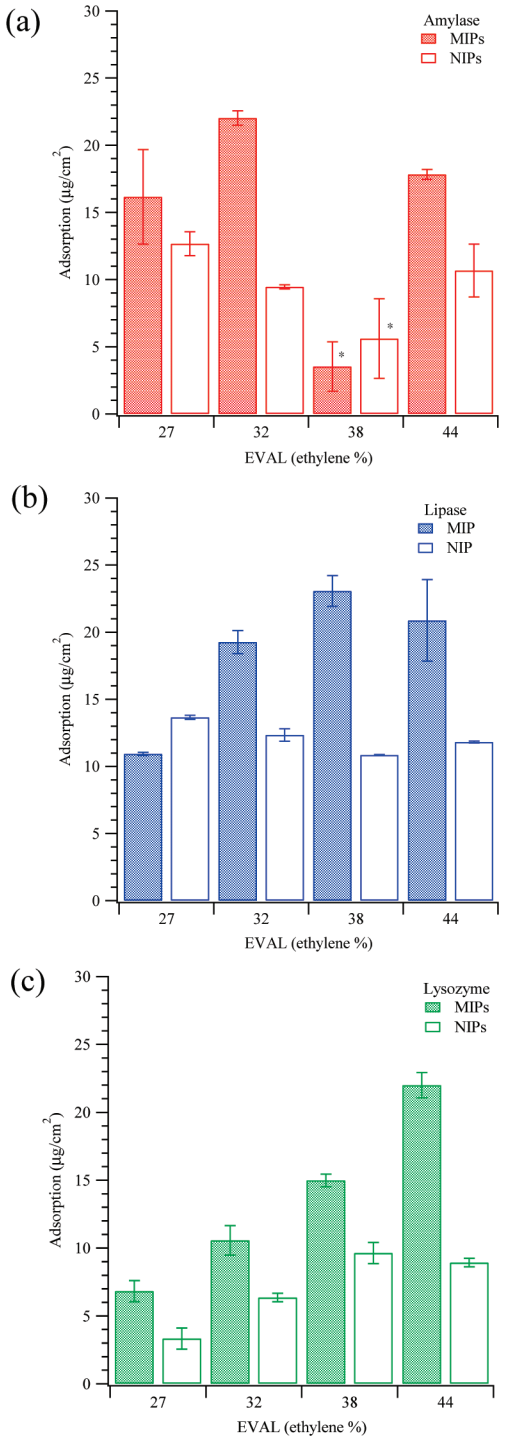

Figure 1. Adsorption capacities of (a) amylase-, (b) lipase-, (c) lysozyme- and nonimprinted EVAL polymers with different mol % of ethylene contents when those salivary protein concentrations are 0.1 mg/mL. Measurements of the depletion from the binding solution were made using UV/vis spectroscopy. *The anomalously low binding to this composition was likely caused by moisture during solidification of EVALs (as no other imprinted films gave lower binding than nonimprinted films); we include this data for completeness.

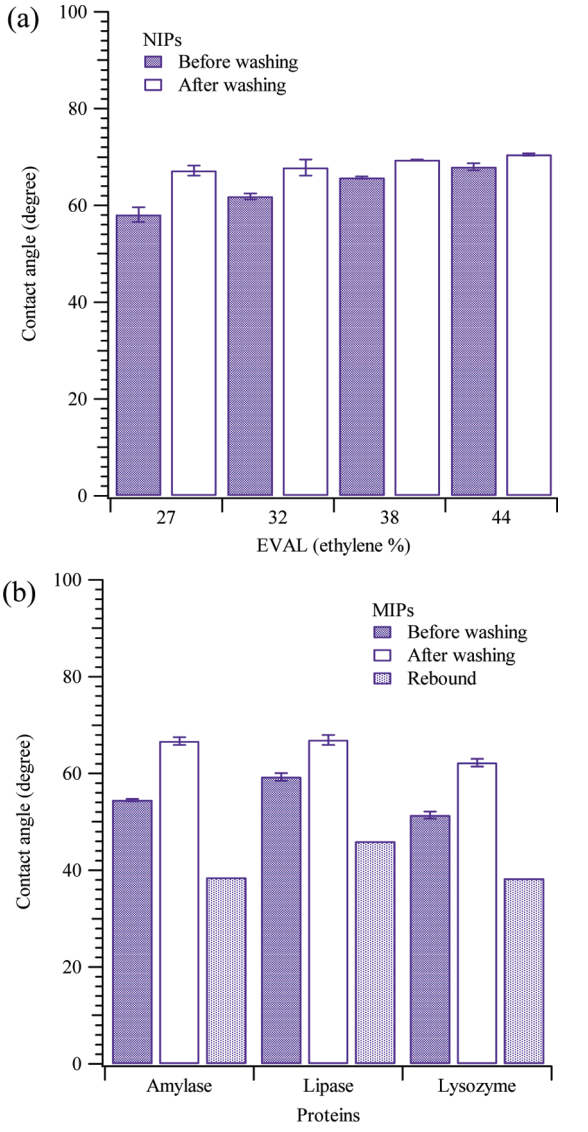

Figure 2. Contact angle measurements on the (a) nonimprinted EVAL (containing different mole % of ethylene) thin films before and after washing and (b) amylase-imprinted EVAL (ethylene mole % is corresponding the prescreening) thin films before and after the template removal, and after rebinding of template molecules.

during the setting of the film.) As the films are typically ~100 μm thick, such porosity can greatly increase the binding capacity. In spite of the uncertainties inherent in these measurements, we believe they remain useful for determining optimal compositions, as films of the same composition will likely show similar binding behavior when placed on QCM chips.

The causes of high nonspecific binding to NIPs (and binding of irrelevant targets to MIPs) is a subject of (a separate) current study, by imprinting individual amino acids and comparing binding to MIPs and NIPs. Undoubtedly, some of the recognition capability of EVAL originates from hydrogen bonding to specific functional groups; even in a nonimprinted film, several functional groups may cooperate to bind simply by chance.

Figure 2 shows the water contact angles on molecularly imprinted and nonimprinted EVALs. The contact angles for EVALs containing ethylene from 27 to 44 mol % are from 58.1 to 68.0 degrees for NIPs; there is a very small increase (<10°) in contact angle after washing, which may be caused by slight surface reorganization leading to slightly higher hydrophobicity. On imprinted EVAL films, the contact angles before washing are

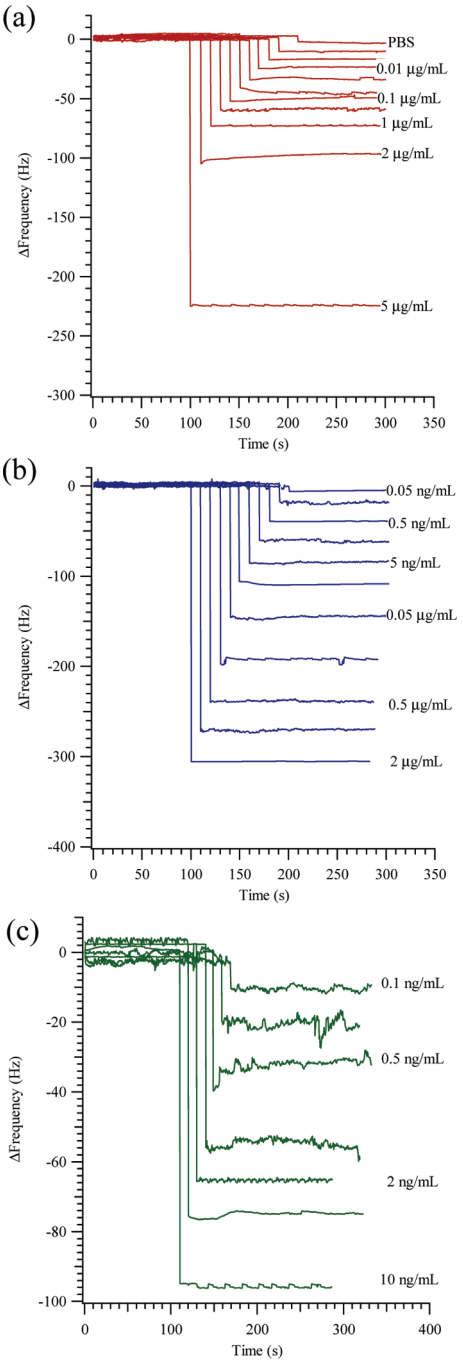

Figure 3. Resonance frequency shift when salivary proteins are adsorbed to (a) amylase-, (b) lipase-, and (c) lysozyme-imprinted EVAL polymeric thin film based QCM sensors.

considerably lower, owing to the hydrophilicity of the template molecules. After washing, the contact angles are similar to those of NIPs, though remaining slightly lower, as is to be expected if some templates remain bound. Rebinding the hydrophilic templates dramatically lowers the contact angles, which is illustrated in the Scheme 1b.

After the effect of the ethylene mole ratio to ethylene alcohol ratio was determined, various concentrations of template protein were measured using a QCM chip with a MIP film made using the proportion of ethylene that was optimal for each specific

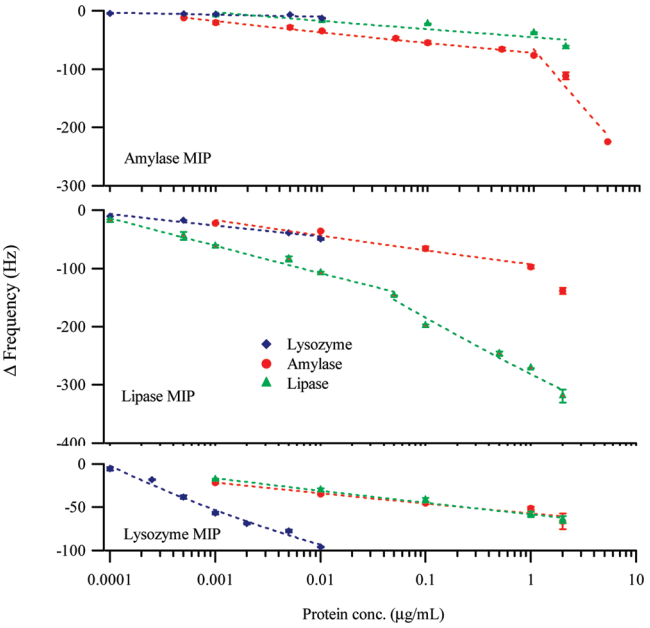

Figure 4. Calibration and interference curves of amylase (red circles); lipase (green triangles) and lysozyme (blue diamonds) to the amylase-, lipase-, and lysozyme-imprinted EVAL polymeric thin film coated QCM chips.

target molecule (32, 38, and 44 mol % ethylene for amylase, lipase, and lysozyme, respectively).

Figure 3 plots the measured frequency changes associated with the addition of target salivary protein solutions to the MIP-QCM sensor. A decrease in the resonance frequency was observed when target molecules were adsorbed by molecularly imprinted EVAL thin films that were coated on the surface of the QCM chip. The saturation of binding by small molecules and micro-organisms in the cavities on the MIP QCM chip reveal that the Langmuir adsorption capacity is larger for smaller molecules. When a large template is used, e.g., microorganisms, the resonant frequency reduction rapidly reaches a plateau. In addition, the QCM chip was placed vertically to prevent the possible precipitation and deposition of microorganisms (though this is not a potential problem with proteins and small molecules). In this work, batchwise adsorption and measurement were performed; therefore, the flow shear effect can be neglected and smaller amounts of samples are required. Moreover, the batchwise experiments may be used to obtain preliminary results for the later integration with a digital microfluidic array. Figure S2 in the Supporting Information displays atomic force microscopic (AFM) images; the surface roughness (listed in Table S3 in the Supporting Information) of the protein-imprinted EVAL thin films after washing and after rebinding is 7.0 and 2.6 nm for amylase; 5.6 and 3.7 nm for lipase; and 2.8 and 1.5 nm for lysozyme, respectively.

The frequency change after each addition stabilized rather rapidly for all three analytes. The binding response is quite rapid (compared with typical biological recognition events); however, the amount bound does saturate as the binding concentration is increased (most apparent for (b) amylase and (c) lysozyme), supporting the interpretation of the frequency shifts as being caused by binding rather than, for example, increased solution viscosity. The maximum frequency fluctuation (noise) in the lysozyme-imprinted EVAL-coated QCM sensor is around 12 Hz. At low amylase concentration, the frequency changes were only

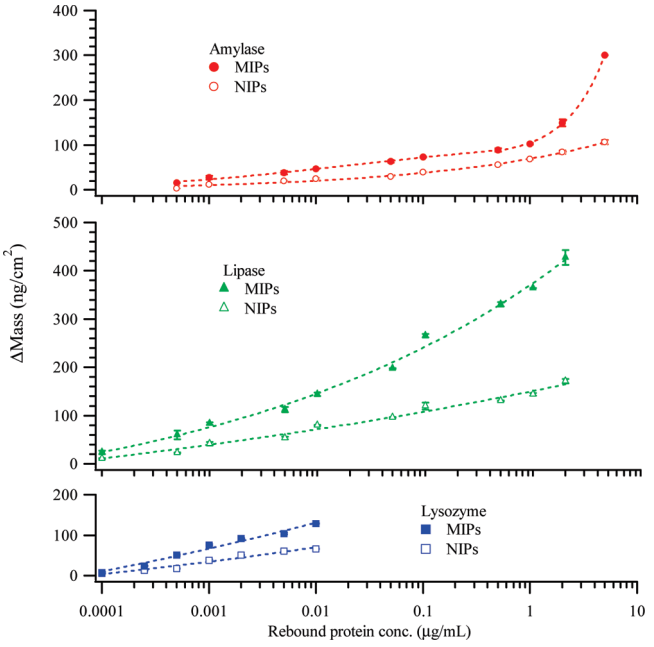

Figure 5. Adsorbed mass of amylase (circles); lipase (triangles) and lysozyme (diamonds) on the amylase-, lipase-, lysozyme-imprinted (filled) and nonimprinted (empty) EVAL polymeric thin film coated QCM chips.

about a quarter of those observed when equal concentrations of lipase and lysozyme in solution were added to lipase- and lysozyme-imprinted EVAL QCM sensors. For example, the frequency changes are about 34.72 ± 1.08, 107.68 ± 2.57, and 96.00 ± 0.50 Hz when 10 ng/mL of amylase, lipase, and lysozyme, respectively, were added.

Figure 4 presents the cross-talk effects of multiple proteins at high concentration. Lipase and lysozyme only weakly affect the amylase-imprinted EVAL QCM sensor when their concentrations are less than 0.5 μg/mL, and the frequency change is also less than 30 Hz. The selectivity of the amylase-imprinted EVAL QCM sensor for the target molecule was two to four times, over the tested interferences. Similar results were also obtained for the lipase-imprinted EVAL QCM sensor. The adsorptions of amylase and lipase by the lysozyme-imprinted EVAL QCM sensor caused very similar frequency changes, perhaps because the template lysozyme molecules were smaller than amylase and lipase molecules, and the smaller cavities may not allow the adsorption of larger molecules. The sensitivities of the amylase-, lipase- and lysozyme-imprinted EVAL QCMs are 10.0, 57.1, and 0.1 mg/mL/Hz, respectively.

The frequency changes associated with the addition of the target salivary proteins to their imprinted and nonimprinted EVAL-coated sensors were converted to the mass changes shown in Figure 5. The limits of detection (LOD) of the MIP QCM sensor are approximately 0.1 mg/mL for all three of the target molecules that were employed in this investigation. The lowest

Table 2. Comparison of Real Sample Measurement by ARCHITECT *ci* 8200 System and the Proposed Protein-Imprinted EVAL QCM Sensor[a]

	ARCHITECT *ci* 8200 system		amylase-MIP QCM Sensor		
sample no.	amylase activity (U/L)	concentration (mg/mL)	Δfrequency (Hz)	concentration (mg/mL)	accuracy (%)
1	34200 ± 1700	1.07 ± 0.06	−76.81 ± 1.49	1.01 ± 0.05	95.28
2	83500 ± 2500	2.75 ± 0.09	−139.94 ± 1.32	2.73 ± 0.03	99.27
3	66200 ± 2800	2.16 ± 0.10	−119.91 ± 3.68	2.22 ± 0.09	97.30
4	32500 ± 900	1.01 ± 0.03	−74.06 ± 0.80	0.91 ± 0.03	90.10
5	54300 ± 3500	1.75 ± 0.12	−111.24 ± 2.97	2.00 ± 0.08	87.50
	ARCHITECT *ci* 8200 system		Lipase-MIP QCM Sensor		
sample no.	lipase activity (U/L)	concentration (mg/mL)	Δfrequency (Hz)	concentration (mg/mL)	accuracy (%)
1	4917 ± 197	0.67 ± 0.03	−276.46 ± 0.52	0.73 ± 0.01	91.78
2	4350 ± 250	0.60 ± 0.03	−262.33 ± 6.16	0.65 ± 0.09	92.30
3	4528 ± 82	0.62 ± 0.01	−259.86 ± 1.75	0.61 ± 0.02	98.39
4	4794 ± 342	0.66 ± 0.05	−261.72 ± 2.45	0.64 ± 0.04	96.97
5	3975 ± 151	0.55 ± 0.02	−254.32 ± 2.66	0.54 ± 0.03	98.18
			lysozyme-MIP QCM sensor		
sample no.	ARCHITECT *ci* 8200 system		Δfrequency (Hz)	concentration (μg/mL)	
1	-	-	−26.60 ± 1.87	0.30 ± 0.03	
2	-	-	−35.00 ± 0.18	0.44 ± 0.01	
3	-	-	−33.14 ± 1.42	0.41 ± 0.03	
4	-	-	−35.83 ± 0.29	0.46 ± 0.01	
5	-	-	−19.36 ± 1.89	0.29 ± 0.02	

[a] The dilution of samples (20 μL) to sensing buffer (2 mL) is 100×.

dx.doi.org/10.1021/am2005724 |*ACS Appl. Mater. Interfaces* 2011, 3, 3064–3071

concentration for positive detection of amylase is around 2 pM. At high amylase concentration (above 1.0 μg/mL), the aggregation of amylase may have caused multilayer adsorption or even precipitation onto the surface of the QCM chip, causing the dramatic change in frequency dissipation that is observed in Figure 3. The effectiveness of imprinting (the ratio of binding on imprinted to binding on nonimprinted films) calculated using the mass changes obtained using the MIP QCM sensor is about a factor of 2, in general agreement with the prescreening results presented in Table 1.

These MIP QCM sensors were then applied for saliva sample measurements. Table 2 summarizes the analyses of five saliva samples from the authors and their colleagues by using an ARCHITECT *ci* 8200 system, which fell in the following ranges: amylase 32500−83500 U/L and lipase 3975−4917 U/L, converted with the calibration curves in the reference.[32] The reference concentrations of amylase and lipase are 1.01−2.75 mg/mL and 0.55−0.67 mg/mL, respectively. The salivary lysozyme concentration is not measured with the ARCHITECT *ci* 8200 system because it is not routine clinical test, but the reference concentration is around 1 μg/mL.[33] According to Table 2, all five salivary samples indicate that the lysozyme concentration is around 0.29−0.46 μg/mL. Their average accuracies for amylase- and lipase-imprinted EVAL QCM sensors are 93.89 and 95.52%.

CONCLUSIONS

In this work, a quartz crystal microbalance (QCM) was utilized to integrate three salivary protein-imprinted EVAL thin films. Those three proteins are digestive proteins that are present high concentrations in saliva and are associated with such diseases as oral cancer and cardiovascular diseases. The optimal ethylene mole ratios of the commercially available EVALs (which yielded the highest imprinting effectiveness at the indicated concentrations) were determined to be 32, 38, and 44 mL % for the imprinting of amylase, lipase and lysozyme, respectively. The limit of detection was compared with those obtained in our earlier studies using molecularly imprinted polymers that were integrated with three transducers - electrochemical, optical and mass-sensitive. The quartz crystal microbalance has a limit of detection of as low as 0.1 ng/mL (ca. 7 pM for lysozyme and 2.5−3.5 pM for lipase and amylase). Finally, the amylase and lipase concentrations of the saliva samples were measured using the MIP QCM sensor and the accuracy of the converted concentrations exceeded 90%, whose value is similar to that for commercial instruments. This demonstrates that the MIP QCM sensor may be both feasible and economical for assessing protein content in biological fluids.

ASSOCIATED CONTENT

Supporting Information. Additional table. This material is available free of charge via the Internet at http://pubs.acs.org.

AUTHOR INFORMATION

Corresponding Author

*Tel: (O) +886(7)591-9455; (M) +886(912)178-751. E-mail: linhy@ntu.edu.tw or linhy@caa.columbia.edu.

ACKNOWLEDGMENT

The authors appreciate the National Science Council of the Republic of China, Taiwan, for financially supporting this research under Contract NSC 100-2220-E-390-001- and NSC 100-2220-E-006-013-.

REFERENCES

(1) Wu, R.; Hu, L.; Wang, F.; Ye, M.; Zou, H. *J. Chromatogr., A* **2008**, *1184*, 369–392.
(2) Lasáková, M.; Jandera, P. *J. Sep. Sci.* **2009**, *32*, 799–812.
(3) Potyrailo, R. A.; Mirsky, V. M. *Chem. Rev.* **2008**, *108*, 770–813.
(4) Holthoff, E. L.; Bright, F. V. *Anal. Chim. Acta* **2007**, *594*, 147–161.
(5) Mayes, A. G.; Whitcombe, M. J. *Adv. Drug Delivery Rev.* **2005**, *57*, 1742–1778.
(6) Rubinstein, I.; Steinberg, S.; Tor, Y.; Shanzer, A.; Sagiv, J. *Nature* **1988**, *332*, 426–429.
(7) Ávila, M.; Zougagh, M.; Ríos, Á.; Escarpa, A. *TrAC, Trends Anal. Chem.* **2008**, *27*, 54–65.
(8) Seidler, K.; Polreichová, M.; Lieberzeit, P.; Dickert, F. *Sensors* **2009**, *9*, 8146–8157.
(9) Jenik, M.; Schirhagl, R.; Schirk, C.; Hayden, O.; Lieberzeit, P.; Blaas, D.; Paul, G.; Dickert, F. L. *Anal. Chem.* **2009**, *81*, 5320–5326.
(10) Jenik, M.; Seifner, A.; Lieberzeit, P.; Dickert, F. *Anal. Bioanal. Chem.* **2009**, *394*, 523–528.
(11) Seifner, A.; Lieberzeit, P.; Jungbauer, C.; Dickert, F. L. *Anal. Chim. Acta* **2009**, *651*, 215–219.
(12) Lin, T.-Y.; Hu, C.-H.; Chou, T.-C. *Biosens. Bioelectron.* **2004**, *20*, 75–81.
(13) Lin, H.-Y.; Hsu, C.-Y.; Thomas, J. L.; Wang, S.-E.; Chen, H.-C.; Chou, T.-C. *Biosens. Bioelectron.* **2006**, *22*, 534–543.
(14) Lee, M.-H.; Thomas, J. L.; Tasi, S.-B.; Liu, B.-D.; Lin, H.-Y. *J. Nanosci. Nanotechnol.* **2009**, *9*, 3469–3477.
(15) Ge, Y.; Turner, A. P. F. *Trends Biotechnol.* **2008**, *26*, 218–224.
(16) Lin, H.-Y.; Ho, M.-S.; Lee, M.-H. *Biosens. Bioelectron.* **2009**, *25*, 579–586.
(17) Lee, M.-H.; Thomas, J. L.; Ho, M.-H.; Yuan, C.; Lin, H.-Y. *ACS Appl. Mater. Interfaces* **2010**, *2*, 1729–1736.
(18) Huang, C.-Y.; Tsai, T.-C.; Thomas, J. L.; Lee, M.-H.; Liu, B.-D.; Lin, H.-Y. *Biosens. Bioelectron.* **2009**, *24*, 2611–2617.
(19) Brosky, M. E. *J. Support Oncol.* **2007**, *5*, 215–225.
(20) Shpitzer, T.; Bahar, G.; Feinmesser, R.; Nagler, R. *J. Cancer Res. Clin. Oncol.* **2007**, *133*, 613–617.
(21) Yap, L. F.; Jenei, V.; Robinson, C. M.; Moutasim, K.; Benn, T. M.; Threadgold, S. P.; Lopes, V.; Wei, W.; Thomas, G. J.; Paterson, I. C. *Oncogene* **2009**, *28*, 2524–2534.
(22) Adam, D. J.; Milne, A. A.; Evans, S. M.; Roulston, J. E.; Lee, A. J.; Ruckley, C. V.; Bradbury, A. W. *J. Vasc. Surg.* **1999**, *30*, 229–235.
(23) Streckfus, C.; Bigler, L. *Oral Dis.* **2002**, *8*, 69–76.
(24) Callegari, C.; Lami, F. *Gut* **1984**, *25*, 909.
(25) Leslie, M. D.; Dische, S. *Radiother. Oncol.* **1994**, *30*, 26–32.
(26) Meyer, P.; Zechel, T. *HNO* **2001**, *49*, 626–629.
(27) Janket, S.-J.; Meurman, J. H.; Nuutinen, P.; Qvarnstrom, M.; Nunn, M. E.; Baird, A. E.; Van Dyke, T. E.; Jones, J. A. *Arterioscler. Thromb. Vasc. Biol.* **2006**, *26*, 433–434.
(28) Qvarnstrom, M.; Janket, S.-J.; Jones, J. A.; Jethwani, K.; Nuutinen, P.; Garcia, R. I.; Baird, A. E.; Van Dyke, T. E.; Meurman, J. H. *J. Clin. Periodontol.* **2010**, *37*, 805–811.
(29) Bikerman, J. *Ind. Eng. Chem., Anal. Ed.* **1941**, *13*, 443–444.
(30) Sreekumar, A.; Poisson, L. M.; Rajendiran, T. M.; Khan, A. P.; Cao, Q.; Yu, J.; Laxman, B.; Mehra, R.; Lonigro, R. J.; Li, Y.; Nyati, M. K.; Ahsan, A.; Kalyana-Sundaram, S.; Han, B.; Cao, X.; Byun, J.; Omenn, G. S.; Ghosh, D.; Pennathur, S.; Alexander, D. C.; Berger, A.; Shuster, J. R.; Wei, J. T.; Varambally, S.; Beecher, C.; Chinnaiyan, A. M. *Nature* **2009**, *457*, 910–914.

(31) Holmes, E.; Loo, R. L.; Stamler, J.; Bictash, M.; Yap, I. K. S.; Chan, Q.; Ebbels, T.; De Iorio, M.; Brown, I. J.; Veselkov, K. A.; Daviglus, M. L.; Kesteloot, H.; Ueshima, H.; Zhao, L.; Nicholson, J. K.; Elliott, P. *Nature* **2008**, *453*, 396–400.
(32) Lee, M.-H.; Chen, Y.-C.; Ho, M.-H.; Lin, H.-Y. *Anal. Bioanal. Chem.* **2010**, *397*, 1457–1466.
(33) Virella, G.; Goudswaard, J. *J. Dent. Res.* **1978**, *57*, 326–328.